An analysis of stable extrapolation operators with absorbing boundaries

Daniel Rothman and Jeff Thorson

Abstract

The range of stable boundary conditions for finite difference wave extrapolation are defined analytically for any degree of approximation of the exact paraxial wave equation, given constant velocity. Eigenvalues and eigenvectors of stable extrapolation operators are presented, along with a numerical study of reflection coefficients arising from imperfectly absorbing boundaries.

Introduction

Finite difference migration or modeling requires the specification of boundary conditions at the sides of the computational grid. The familiar zero-slope (Neumann) or zero-value (Dirichlet) end conditions unfortunately result in artificial side boundary reflections when waves are incident at the boundary. Consequently, absorbing boundary conditions were developed which attenuate or virtually eliminate these reflections (Clayton and Engquist, 1980; Toldi and Hale, 1982).

Stability of the wave extrapolation operator remains a necessity with the inclusion of absorbing boundary conditions. Clayton and Engquist (1980) proved that stability exists with the 15 degree approximation of the paraxial wave equation and the use of a particular form for absorbing boundaries. A relatively simple algebraic proof is presented here that establishes the range of stable boundary conditions with any degree of approximation of the exact paraxial wave equation, in a medium of constant velocity. Stability is proven through an analysis of the eigenvalues of the extrapolation operator, and computed eigenvalues and eigenvectors of operators with reflecting and absorbing boundaries are illustrated.

Absorbing boundary conditions may still reflect waves; the strength of the reflection depends, in general, upon the incident angle of the wave at the boundary. This paper illustrates the reflection coefficients of side boundaries, which have been empirically determined as a function of incident angle for reflecting and absorbing boundary conditions.

Review

The scalar wave equation for the downward extrapolation of a wavefield **q** is

$$\frac{\partial \mathbf{q}}{\partial z} = ik_z \mathbf{q} = -\mathbf{R}\mathbf{q}, \tag{1}$$

where **R** takes the form (for constant ω and v)

$$-ik_z = -i\frac{\omega}{v}\sqrt{1 - v^2\frac{k_x^2}{\omega^2}}.$$

Our concern is with the stability of differential equation (1); that is, we desire that its solution $\mathbf{q}_z = e^{-\mathbf{R}z}q_0$ does not grow with increasing z. Clearly this depends upon the eigenvalues $\lambda(\mathbf{R})$ of **R**. Stability will hold if $\mathrm{Re}\{\lambda(\mathbf{R})\} \geq 0$. Our form of extrapolation, of course, is performed with difference equations, not differential equations. Going to the discrete domain does not change the conditions for stability, however, as the same limitations must still be placed on the eigenvalues of **R** (Godfrey et al, 1979). Since our primary interest lies with these eigenvalues, we will explicitly define the eigenvalues of the matrix components of **R**.

R is conveniently expressed as $\mathbf{R} = \mathbf{V}^{-1/2}\mathbf{M}\mathbf{V}^{-1/2}$, where **M** is a continued fraction containing matrices $\mathbf{D}_t$, **V**, and **T**,

$$\mathbf{M} = \mathbf{D}_t + \cfrac{\mathbf{VTV}}{2\mathbf{D}_t + \cfrac{\mathbf{VTV}}{2\mathbf{D}_t + \cfrac{\mathbf{VTV}}{2\mathbf{D}_t + \cdots}}} \tag{2}$$

$\mathbf{D}_t$ is a time derivative operator, $\mathbf{D}_t = (\varepsilon + i\omega)\mathbf{I}$, where **I** is the identity matrix and $\varepsilon \geq 0$ and real. $\mathbf{V} = v_0\mathbf{I}$, v_0 being the constant velocity of the medium. **T** is a second spatial derivative operator. Following Thorson (1979), we can add a complex perturbation p to the upper left and lower right corner elements of the differencing matrix to represent the inclusion of absorbing boundary conditions. The zero slope condition is then $p = 0$, and the zero value condition is $p = 1$. **T** is therefore defined as

$$\mathbf{T} = \frac{1}{\Delta x^2}\begin{bmatrix} (1+p) & -1 & & & \\ -1 & 2 & -1 & & \\ & \bullet & & & \\ & & \bullet & & \\ & & -1 & 2 & -1 \\ & & & -1 & (1+p) \end{bmatrix}.$$

Note that truncating **M** in equation (2) before the third **VTV** leads to the 45° extrapolation equation, while its infinite continuation represents the 90° equation. We will define a range of stable absorbing boundary conditions (stable values of p) for the infinite continuation of **M**; thus, for the exact paraxial wave equation.

Two fundamental observations

Before stating the stability proof we make two observations from elementary linear algebra.

Observation 1. If a matrix **A** exists such that $\mathrm{Re}\{\mathbf{x}^H\mathbf{A}\mathbf{x}\} \geq 0$ for any vector x, then $\mathrm{Re}\{\lambda(\mathbf{A})\} \geq 0$ (superscript H denotes conjugate transpose).

Proof. Since **x** is arbitrary, let it be an eigenvector of **A**. Then

$$\mathrm{Re}\{\mathbf{x}^H\mathbf{A}\mathbf{x}\} = \mathrm{Re}\{\mathbf{x}^H\lambda\mathbf{x}\} = \mathrm{Re}\{\mathbf{x}^H\mathbf{x}\lambda\} \geq 0.$$

$\mathrm{Re}\{\lambda(\mathbf{A})\} \geq 0$ for the equation to hold, therefore the observation is proven.

Observation 2. If **N** is a normal matrix (normal matrices are those matrices that commute with their conjugate transpose, so that $\mathbf{N}^H\mathbf{N} = \mathbf{N}\mathbf{N}^H$) and $\mathrm{Re}\{\lambda(\mathbf{N})\} \geq 0$, then $\mathrm{Re}\{\mathbf{x}^H\mathbf{N}\mathbf{x}\} \geq 0$ for any **x**.

Proof. Since N is normal, it possesses a linearly independent set of orthonormal eigenvectors $\mathbf{x}_i$, and any arbitrary **x** can be written as the linear combination $c_1\mathbf{x}_1 + \ldots + c_n\mathbf{x}_n$. Then

$$\mathbf{N}\mathbf{x} = c_1\mathbf{A}\mathbf{x}_1 + \ldots + c_n\mathbf{A}\mathbf{x}_n$$

$$= c_1\lambda_1\mathbf{x}_1 + \ldots + c_n\lambda_n\mathbf{x}_n .$$

Orthonormality of the eigenvectors $\mathbf{x}_i$ means that

$$\mathbf{x}_i^H\mathbf{x}_j = \begin{cases} 1 & i=j \\ 0 & else \end{cases}$$

Thus we have

$$\mathrm{Re}\{\mathbf{x}^H\mathbf{N}\mathbf{x}\} = \mathrm{Re}\{ (c_1^H\mathbf{x}_1^H + \ldots + c_n^H\mathbf{x}_n^H)(c_1\lambda_1^H\mathbf{x}_1 + \ldots + c_n\lambda_n^H\mathbf{x}_1) \}$$

$$= \mathrm{Re}\{ |c_1|^2\lambda_1 + \ldots + |c_n|^2\lambda_n \}$$

Therefore, if $\mathrm{Re}\{\lambda(\mathbf{N})\} \geq 0$, then $\mathrm{Re}\{\mathbf{x}^H\mathbf{N}\mathbf{x}\} \geq 0$ for any **x**.

The stability proof

We rewrite equation (2) as suggested by Francis Muir in a recent lecture to the SEP,

$$\mathbf{M} = \frac{\mathbf{L}_1}{2} + \cfrac{1}{\mathbf{L}_1 + \cfrac{1}{\mathbf{L}_2 + \cfrac{1}{\mathbf{L}_1 + \cdots}}} \tag{3}$$

where $\mathbf{L}_2 = 2\mathbf{D}_t$ and $\mathbf{L}_1 = \frac{\mathbf{L}_2}{\mathbf{VTV}}$. Since stability depends directly on the eigenvalues of **R**, we will first establish bounds for the eigenvalues of **M**, and $\lambda(\mathbf{R})$ will then be obtainable directly.

The eigenvalues of **M** can be determined from the eigenvalues of $\mathbf{L}_1$ and $\mathbf{L}_2$ by simply replacing the matrices in equation (3) with their respective eigenvalues. This is an allowable substitution because (1) the matrices $\mathbf{L}_1$ and $\mathbf{L}_2$ share the same set of eigenvectors, and (2) $\mathbf{L}_1$ and $\mathbf{L}_2$ are diagonalizable. The former condition is immediately apparent; $\mathbf{L}_2$ is just a (complex) constant times **I**, and therefore it shares eigenvectors with all matrices of equal dimensions. Condition (2) does not come quite so easily. $\mathbf{L}_2$ is already diagonal, but $\mathbf{L}_1$ must contain a full set of linearly independent eigenvectors. This will be assumed. ($\mathbf{L}_1$ *is* diagonalizable for $p = 0$. Since p represents only a small perturbation of $\mathbf{L}_1$ the assumption is valid).

We want that $\mathrm{Re}\{\lambda(\mathbf{M})\} \geq 0$, since this will imply the stability of **R**. This will be true if the eigenvalues of $\mathbf{L}_1$ and $\mathbf{L}_2$ are (semi-) positive real, since the reciprocals of positive real numbers are positive real, and the sum of positive reals is positive real. Since $\mathbf{L}_2$ is positive real by definition ($\varepsilon \geq 0$), all that remains to establish are the limitations on p such that the eigenvalues of $\mathbf{L}_1$ have positive real parts.

T can be decomposed such that $\mathbf{T} = \frac{1}{\Delta x^2}(\mathbf{T}_0 + \mathbf{P})$ (Thorson, 1979),

$$\mathbf{T}_0 = \begin{bmatrix} 1 & -1 & & & \\ -1 & 2 & -1 & & \\ & \ddots & & \ddots & \\ & & -1 & 2 & -1 \\ & & & -1 & 1 \end{bmatrix}, \qquad \mathbf{P} = \begin{bmatrix} p & & & \\ & \textit{zeros} & & \\ & & & p \end{bmatrix}.$$

This decomposition allows us to exploit two characteristics of $\mathbf{T}_0$ and **P**. Both are normal matrices, and $\mathrm{Re}\{\lambda(\mathbf{T}_0)\} \geq 0$ †. Let us assume also that $\mathrm{Re}\{p\} \geq 0$, providing that $\mathrm{Re}\{\lambda(\mathbf{P})\} \geq 0$. Then, by Observation 2, $\mathrm{Re}\{\mathbf{x}^H\mathbf{T}_0\mathbf{x}\} \geq 0$ and $\mathrm{Re}\{\mathbf{x}^H\mathbf{P}\mathbf{x}\} \geq 0$, and by

† The eigenvalues of $\mathbf{T}_0$ can be found in many linear algebra texts, but Gershgorin's theorem (Strang, 1980) provides the needed information quite simply.

addition, $\mathrm{Re}\{\mathbf{x}^H\mathbf{T}\mathbf{x}\} \geq 0$. Observation 1 now allows us to conclude that $\mathrm{Re}\{\lambda(\mathbf{T})\} \geq 0$. Pre- and post-multiplication by **V** only acts to scale the eigenvalues by v_0^2, and therefore $\mathrm{Re}\{\lambda(\mathbf{VTV})\} \geq 0$.

Letting $\lambda(\mathbf{VTV}) = \alpha + i\beta$, we have

$$\lambda(\mathbf{L}_1) = \frac{\varepsilon + i\omega}{\alpha + i\beta} = \frac{\varepsilon\alpha + \beta\omega + i(\alpha\omega - \varepsilon\beta)}{\alpha^2 + \beta^2}$$

The above quantity will be positive real if $\varepsilon\alpha \geq 0$ and if $sgn(\omega) = sgn(\beta) = sgn(\mathrm{Im}\{p\})$. The former condition holds due to our definition of ε and our assumption for p, while the latter case is true at our discretion. Thus $\lambda(\mathbf{L}_1)$ and $\lambda(\mathbf{L}_2)$ are positive real, implying that $\lambda(\mathbf{M})$ is positive real. Since multiplication by the square root of the velocity matrix will not affect the sign of the eigenvalues, $\mathrm{Re}\{\lambda(\mathbf{R})\} \geq 0$. Therefore, **R** is a stable operator if $\mathrm{Re}\{p\} \geq 0$ and $sgn(\omega) = sgn(\mathrm{Im}\{p\})$.

The eigenvalues and eigenvectors

In the Crank-Nicolson implementation of equation (1) operator **R** takes the form **R′**

$$\mathbf{R}' = \frac{\mathbf{I} - \frac{\Delta z}{2}\mathbf{R}}{\mathbf{I} + \frac{\Delta z}{2}\mathbf{R}}$$

In order to gain increased accuracy of the second spatial derivative, the "1/6 trick" (Claerbout, 1982) may be used to redefine **T** as **T′**.

$$\mathbf{T}' = \frac{\mathbf{T}}{\mathbf{I} + \frac{\Delta x^2}{6}\mathbf{T}}$$

The eigenvalues and eigenvectors of **R′** are displayed in Figs. 1 - 4. **M** was truncated to form the 45° extrapolation operator, **T** was chosen to equal **T′**, and the constants chosen were $\varepsilon = 0$, $\omega = \pi$, $v_0 = 1$, $\Delta z = 1$, and $\Delta x = 1$. The x-direction has been discretized over 32 points, so **R′** is a 32 by 32 matrix. Figures 1 and 2 show the eigenvalues and eigenvectors for the case $p = 0$. The eigenvalues are distributed on a portion of the unit circle, because the eigenvalues of **T** are purely real and $\varepsilon = 0$. Note that the eigenvectors of **R′** are also the eigenvectors of **T**. The eigenvectors essentially represent different k_x components of operator **R′**, from $k_x = 0$ to $k_x = \pi$ (Nyquist). The wave propagation angles spanned by the eigenvectors range from 0 to 90 degrees.

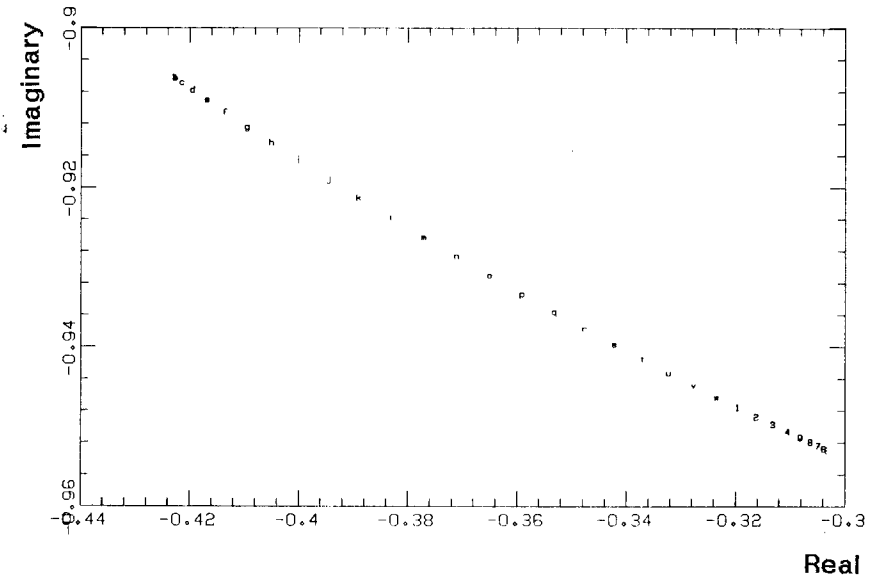

FIG. 1. Eigenvalues of **R′** for $p = 0$ plotted in the complex plane. The real axis is horizontal, the imaginary vertical. The eigenvalues are distributed along a portion of the unit circle; note the different scales of each axis. The eigenvalues were plotted and labeled in the order a-w,1-9.

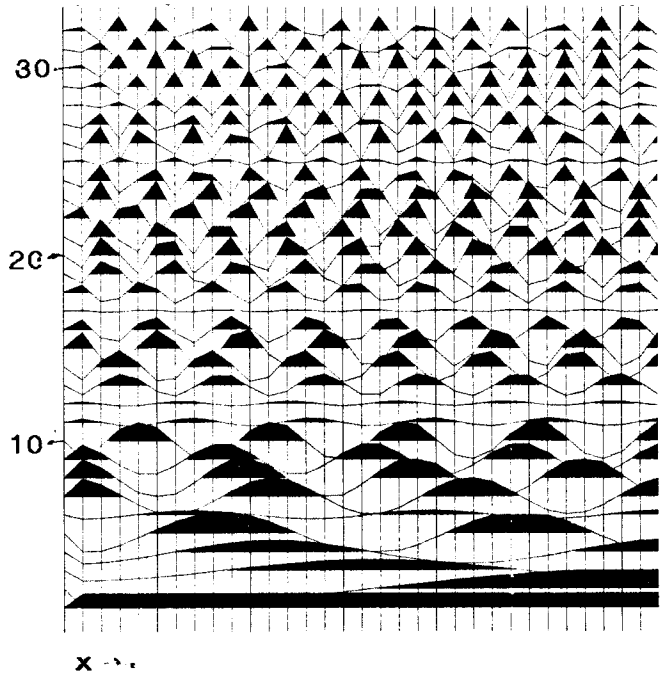

FIG. 2. Eigenvectors of **R′** for $p = 0$. The eigenvectors are purely real. Each horizontal trace represents an eigenvector. Eigenvectors correspond to the eigenvalues of Fig. 1 as follows: the bottommost eigenvector corresponds to eigenvalue "a", while the topmost vector corresponds to value "9".

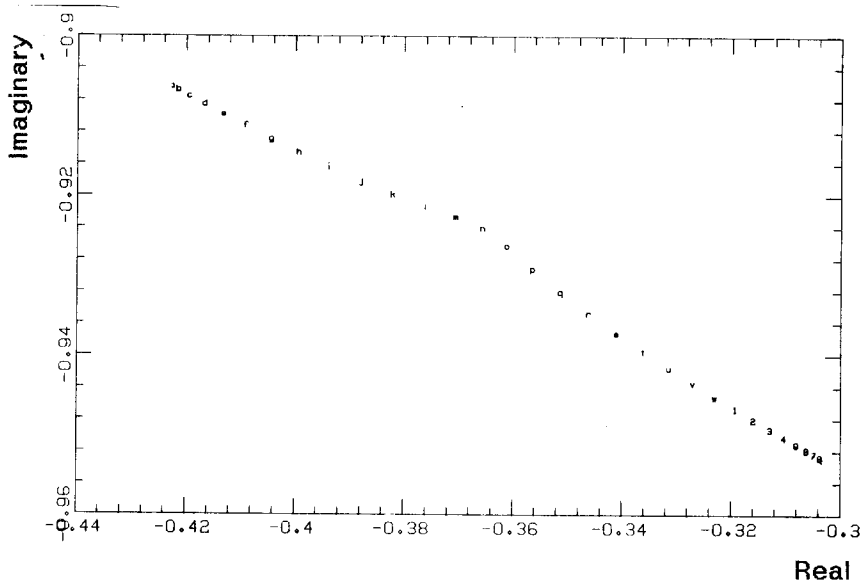

FIG. 3. Eigenvalues of **R′** for $p = .7630 + .9715i$, the B1 boundary condition designed to fully attenuate reflections for waves incident at 30°. The eigenvalues are now inside the unit circle.

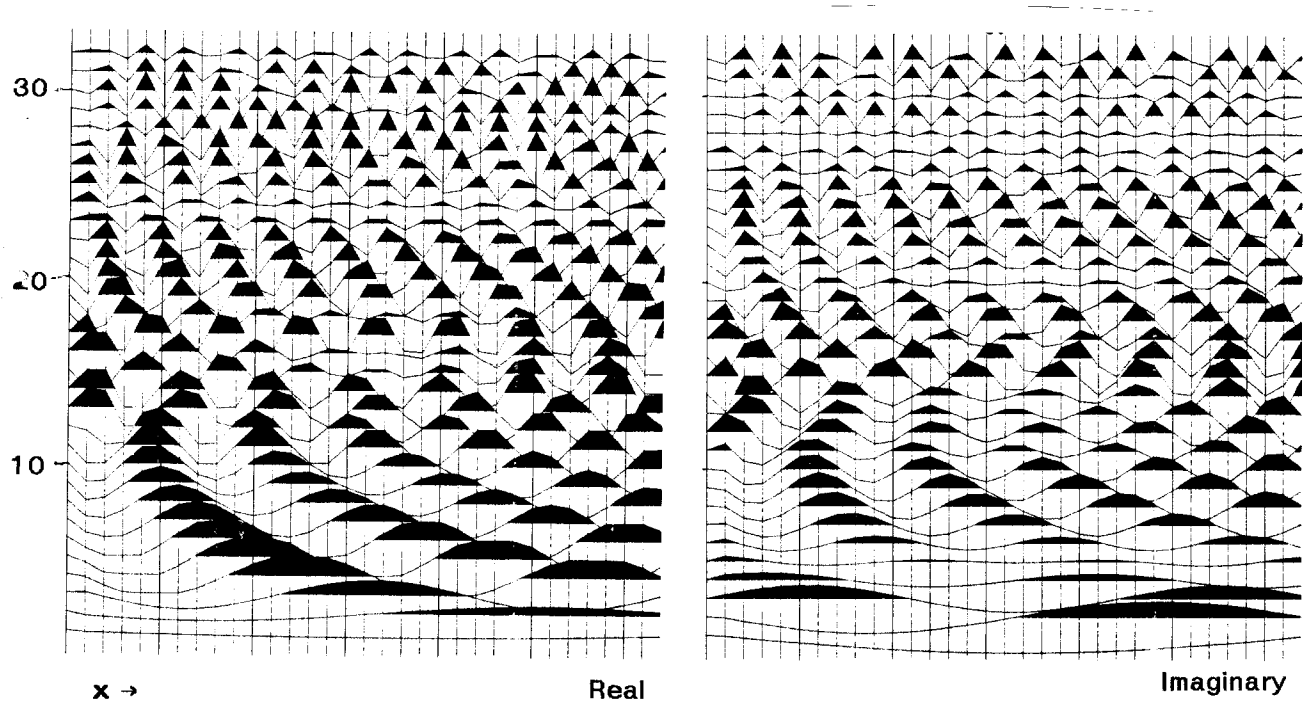

FIG. 4. Eigenvectors of **R′** for $p = .7630 + .9715i$. The real part of the eigenvectors is shown on the left, the imaginary on the right. The eigenvector-eigenvalue correspondence of Figs. 3 and 4 is the same as in Figs. 1 and 2.

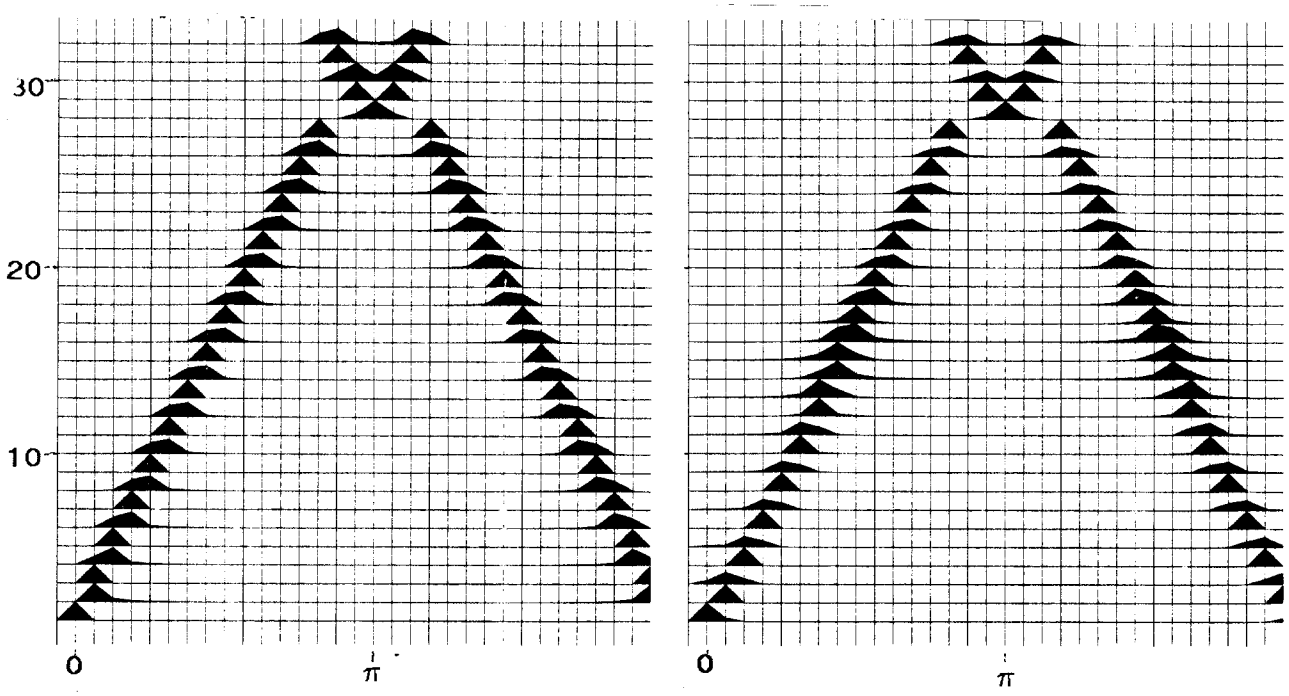

FIG. 5. Fourier spectra of the eigenvectors in Figs. 2 and 4. The case $p = 0$ is shown on the left. Each horizontal trace is the spectrum of its corresponding eigenvector in the previous figures. Vertical lines denote the placement of each sample output from the FFT. $k_x = \pi = Nyquist$ is in the center and negative frequencies are on the right side of each plot. Note the relative smearing in the spectra near $k_x = \pm\frac{\pi}{2}$ in the diagram on the right.

Figures 3 and 4 illustrate the case $p = .7630 + .9715i$. This p-value was chosen in accordance with the "B1" absorbing boundary condition of Clayton and Engquist (1980). p was computed such that the side reflections of waves incident at the boundary with an angle of 30° at either side are fully attenuated. The eigenvalues have noticeably moved to within the unit circle due to the absorbing boundary condition, indicating that the energy of waves will dissipate as they propagate downward to infinity, losing energy with each side boundary reflection. The eigenvectors reveal changes also, but the differences are not as clearly perceptible. In order to quantify the differences, the Fourier spectra of both eigenvector sets were computed and are displayed in Figure 5. Notice that the eigenvectors containing the 9th and 24th spectral components (and neighboring components) exhibit less sharply defined spectra after the inclusion of absorbing boundaries. This is precisely where we expect to see the changes, since $\sin\theta_{absorbing} = \frac{vk_x}{\omega} = \pm 1/2$ implies that the eigenvectors corresponding to $k_x = \pm\frac{\pi}{2}$ will be most affected.

Reflection coefficients

Clayton and Engquist (1980) derived analytic expressions for the reflection coefficients arising from absorbing boundaries. As a matter of practical interest, we provide an empirical evaluation of reflection coefficients for the zero slope and B1 boundary conditions.

Boundary reflections were attained by downward continuing plane waves with the 45 degree version of R′ described in the previous section, once for each of the 32 values of k_x. We expect that the input wave, e^{ik_x}, equals a reflection coefficient times the reflected wave, re^{-ik_x}. The Fourier spectrum of the downward continued wave was compared to the spectrum of the input plane wave, and the reflection coefficient r was computed as the square root of the ratio of the spectral values $\frac{k_{x(out)}}{k_{x(in)}}$.

Figures 6 and 7 illustrate the reflection coefficient as a function of incident angle for both boundary conditions. Although the reflection coefficient for the zero slope condition should theoretically be unity for all non-zero angles, the slight discrepancies evident here are probably due to the short (32 point) spatial axis with which computations were made. The B1 boundary condition for Figure 7 was chosen as in the previous section, such that the incident angle of greatest attenuation is $\pm 30°$. Figure 7 exhibits this characteristic; waves incident at 30° are virtually fully attenuated, while waves incident near 30° reflect with substantially reduced amplitude. This graph closely resembles the analytic representation of reflection coefficients shown in Figure 3 of Clayton and Engquist (1980).

Conclusions

A range of stable boundary conditions can be described for a finite difference implementation of any approximation of the exact paraxial wave equation. By defining a parameter p, a perturbation of the second differencing matrix, boundary conditions have been shown to be stable if $\mathrm{Re}\{p\} \geq 0$ and $sgn(\omega) = sgn(\mathrm{Im}\{p\})$. In addition, it has been demonstrated that the inclusion of boundary conditions causes the spectra of the downward continuation operator's eigenvectors to be less sharply defined for those eigenvectors containing the spatial frequencies attenuated on reflected waves. The relative magnitude of these reflections has been determined numerically, and is seen to closely resemble its previous analytic expression.

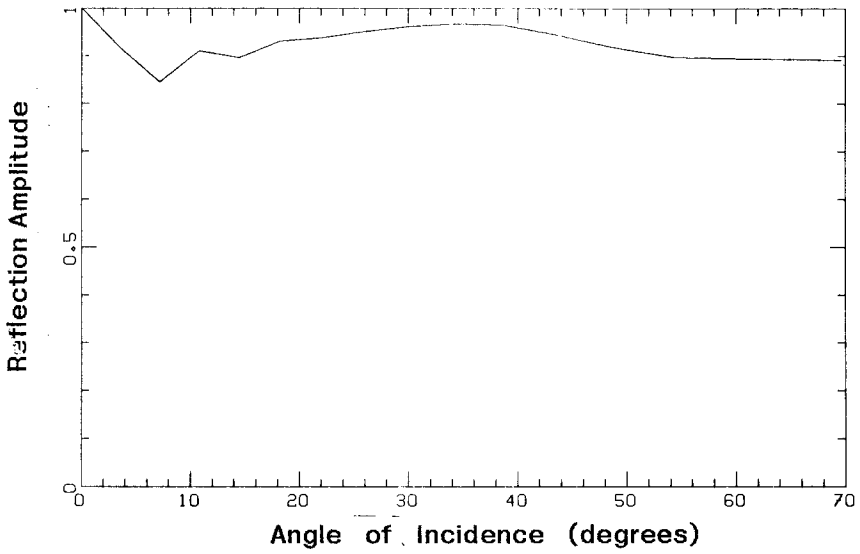

FIG. 6. Reflection coefficient magnitude as a function of incident angle for the zero-slope boundary condition.

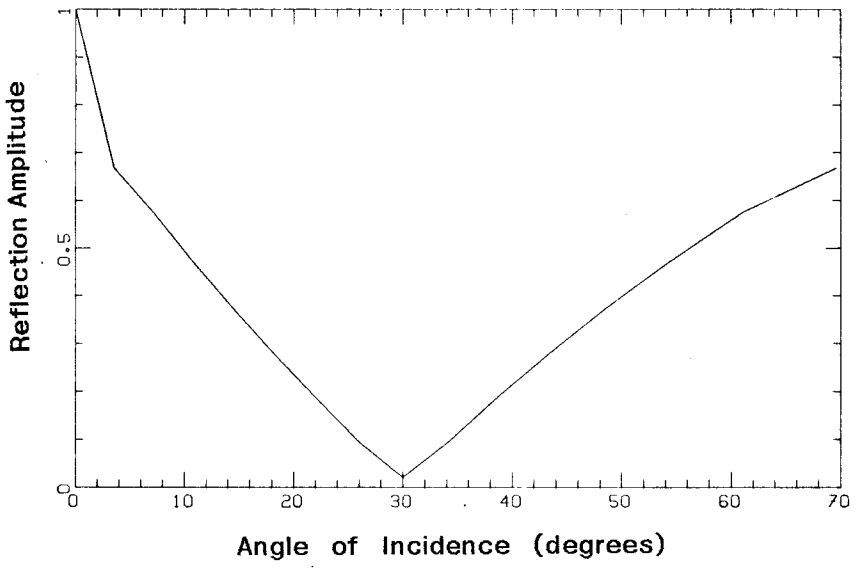

FIG. 7. Reflection coefficient magnitude as a function of incident angle for the B1 boundary condition, designed to fully attenuate reflections of waves incident at 30°.

ACKNOWLEDGMENTS

The authors wish to express their gratitude to Fabio Rocca for suggesting the empirical evaluation of reflection coefficients. We would also like to thank Bert Jacobs and John Toldi for their instructive comments.

REFERENCES

Claerbout, J., 1982, Imaging the earth's interior: SEP Report 30, p.366-367.

Clayton, R. and Engquist, B., 1980, Absorbing side boundary conditions for wave equation migration: Geophysics, v.45, p.895-904.

Godfrey, B., Muir, F., and Claerbout, J., 1979, Stable extrapolation: SEP Report 16, p.83-87.

Strang, G., 1980, Linear algebra and its applications: New York, Academic Press, Inc., p. 304.

Thorson, J., 1979, Stability of finite difference boundary conditions: SEP Report 20, p. 165-178.

Toldi, J. and Hale, D., 1982, Data-dependent absorbing boundaries: SEP Report 30, p. 111-120.

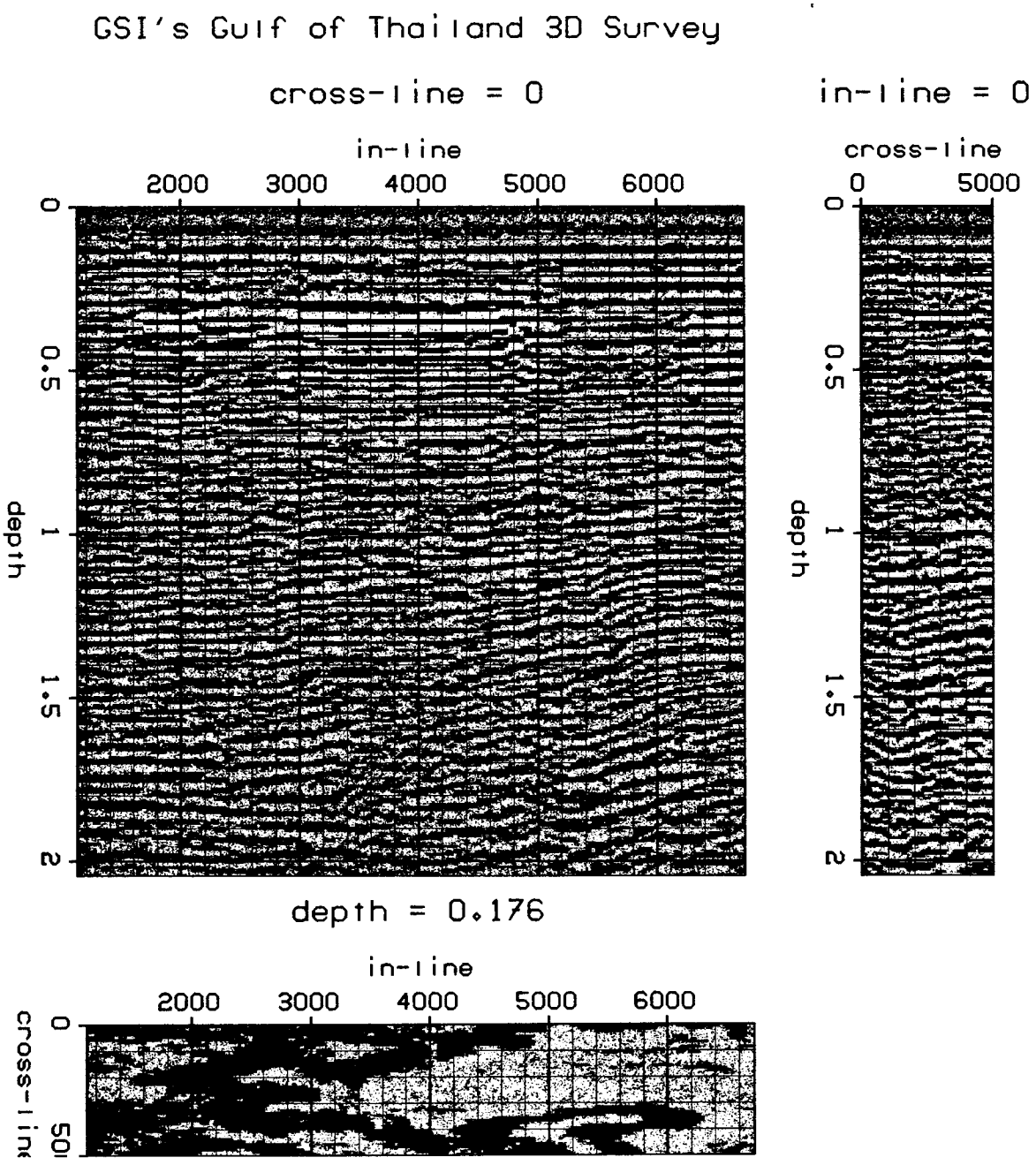
GSI's Gulf of Thailand 3D Survey
cross-line = 0
in-line
2000
3000
4000
5000
6000
0
0.5
1
1.5
2
depth
in-line = 0
cross-line
0
5000
depth = 0.176
in-line
cross-line